

Propagation in rough waveguides: Forward and inverse problems

M. Spivack*¹ and O. Rath Spivack†¹

¹Department of Applied Mathematics and Theoretical Physics, University of Cambridge, UK

¹Department of Applied Mathematics & Theoretical Physics,
Centre for Mathematical Sciences, University of Cambridge, Cambridge CB3 0WA, UK

Abstract

We discuss here the direct and inverse problems for wave propagation in a waveguide with rough internal surface and arbitrary mean shape. The high degree of multiple scattering inside the waveguide poses significant challenges both for the forward computation and for the recovery of the surface profile, and raises important questions about scattering cross-sections. This paper falls into two parts corresponding to these issues.

We first apply Left-Right (L-R) operator splitting to calculate the scattered fields in 2- and 3-dimensional waveguides. Using this we illustrate the scattered fields and the effect of surface roughness. In the second part we formulate an algorithm for surface recovery from field measurements along the waveguide axis, which generalises recent work on surfaces in 2 dimensions. This method utilizes forward scattering assumptions in effect by formulating an integral equation in the unknown surface field, treated as a function of the surface. Although discussed in the context of waveguides, the formulae are given in a form applicable to a variety of geometries, with coefficients which will depend on and be determined by each specific application.

1 Introduction

Imaging of rough surfaces from acoustic or electromagnetic scattering data is a significant challenge in a wide range of applications, attracting a great deal of attention in various regimes using a variety of approaches [1–12]. However, fewer results are available for rough ducts or waveguides, despite their importance in fields such as biomedical imaging, non-destructive testing, and detection of low cross-section aircraft. The scarcity of results is largely due to the computational and analytical difficulties inherent in calculating fields within extended arbitrarily curved waveguides.

We consider here propagation in a waveguide with a rough internal surface and given arbitrary mean shape, in both 2D and 3D. The study falls into two distinct parts: the forward problem for which we implement an efficient operator splitting approximation previously applied to smooth-sided waveguides; and the inverse problem of profile recovery. For the latter problem, we give, without implementing here, a general formulation which is applicable to a range of geometries having a principal direction of propagation. This reformulates the marching algorithm which has been validated in previous work on 1-dimensional rough surface recovery [12–14]. The algorithm is expressed, for each unknown surface coordinate, as a closed form expression depending explicitly on upstream values. The formula includes

*ms100@cam.ac.uk

†or100@cam.ac.uk

coefficients which are to be determined in the specific regime in which it is applied. Applications will be presented in subsequent work.

Both of these tasks present significant difficulties due to severe computational complexity and a high degree of multiple scattering. However, the predominance of forward scattering can be turned to advantage; Left-Right operator splitting (closely related to the Method of Multiple Ordered Interactions and the Forward-Backward method) proves accurate and efficient and is well-suited to this purpose [15–18].

For the forward problem we calculate scattering for a range of parameters along canonical curved waveguides, with and without surface roughness, in both two and three dimensions. We use this to examine the scattered signal and the effect on this of roughness. Preliminary results are given for individual realisations and ensemble averages. The key features are captured by taking just two terms of the series solution; in fact backscatter is entirely due to the second. The results are intended to be illustrative, and a much wider study is required especially three-dimensions to properly explore cross-polarisation and variation with parameters.

For surface reconstruction using measurements along the duct axis, the proposed algorithm casts the problem as an integral equation in the unknown surface field, treated as a function of the surface, and extends recent work on the recovery of an near-planar 1D surface [13,14]. As mentioned above this yields an expression for each unknown surface coordinate depending explicitly on upstream values, with coefficients to be determined depending on the application.

This paper is organised as follows: The forward problem for a rough-sided 2-dimensional duct is treated in section 2.1 in terms of coupled integral equations following the L-R operator series method of [19,20]. The numerical solution is summarised and computational examples given for an elongated rough duct. In section 2.2 the generalisation to a 3-dimensional rough duct is shown, giving the series solution and example calculations. Finally the inverse problem is discussed in section 3, and the marching or ‘surface sweep’ solution is presented.

2 Propagation in rough waveguides: forward calculation

2.1 Rough two-dimensional waveguide

In this section we consider the propagating fields due to a wave impinging on a (possibly curved) rough-sided 2-dimensional waveguide. The formulation is expressed throughout terms of electromagnetic waves but in this setting reduces to a scalar problem and is equally applicable to acoustics. respectively.

2.1.1 Formulation

The two bounding surfaces are perfectly conducting and denoted S_1 and S_2 . For convenience we summarise here the governing equations and approach from [20] for a smooth canonical waveguide.

The aperture, A , is at the left. The incident field on this aperture may be a horizontally or vertically polarized plane wave (TE or TM, equivalent to Dirichlet or Neumann boundary conditions for an acoustic wave). The field internal to the waveguide is written as a boundary integral over the field induced by the aperture field along its surface. We will assume vertical polarization so the magnetic field H obeys the Helmholtz wave equation $(\nabla^2 + k^2)H = 0$. Let G be the free space Green’s function, so that G is the zero order Hankel function of the first kind,

$$G(\mathbf{r}, \mathbf{r}') = \frac{1}{4i} H_0^{(1)}(k|\mathbf{r} - \mathbf{r}'|). \quad (1)$$

where $\mathbf{r} = (x, z)$ and x and z denote horizontal and vertical coordinates respectively.

The forward problem is to obtain the surface currents along the duct, and from these to calculate the internal fields. The field at a point \mathbf{r} inside the waveguide is written as a boundary integral along

the duct surfaces:

$$H_s(\mathbf{r}) = H_{inc}(\mathbf{r}) + \int_S \left[\frac{\partial G(\mathbf{r}, \mathbf{r}')}{\partial \mathbf{n}} H(\mathbf{r}') \right] dr' \quad (2)$$

where \mathbf{n} denotes the normal outward from the waveguide, $\mathbf{r}_s = (x, S(x))$, $\mathbf{r}' = (x', S(x'))$ and S is the union of the two surfaces. Taking limits as \mathbf{r} tends to the upper and to the lower surfaces and applying boundary conditions, we obtain coupled integral equations in H along the two surfaces. It is convenient to regard these as separate functions of the single coordinate x :

$$J_1(x) = H(x, S_1(x)) , \quad J_2(x) = H(x, S_2(x)). \quad (3)$$

The coupled integral equations for J_1, J_2 can then be written

$$\begin{aligned} H_{inc}(\mathbf{r}_1) &= \int_S [G_{\mathbf{n}}(\mathbf{r}_1; \mathbf{r}'_2) J_2(x') - G_{\mathbf{n}}(\mathbf{r}_1; \mathbf{r}'_1) J_1(x')] dr' \\ H_{inc}(\mathbf{r}_2) &= \int_S [G_{\mathbf{n}}(\mathbf{r}_2; \mathbf{r}'_2) J_2(x') - G_{\mathbf{n}}(\mathbf{r}_2; \mathbf{r}'_1) J_1(x')] dr' \end{aligned} \quad (4)$$

where $G_{\mathbf{n}}$ denotes the normal derivative of G , and $\mathbf{r}_i = (x, S_i(x))$, $\mathbf{r}'_i = (x', S_i(x'))$ for $i = 1, 2$. This set of coupled equations can be solved to find the field terms J_1, J_2 along the surfaces, which may be substituted into equation (2) to yield the value of the field in the waveguide.

For a given external field impinging on the duct, the incident field H_{inc} can be obtained as an integral over the aperture. This represents the field which would exist beyond the aperture, in the absence of the waveguide itself. Here the external field is taken to be a plane wave.

For convenience we now write eq.(4) in operator notation,

$$\begin{aligned} H_{inc}(\mathbf{r}_1) &= (L_{11} + R_{11})J_1 + (L_{12} + R_{12})J_2 \\ H_{inc}(\mathbf{r}_2) &= (L_{21} + R_{21})J_1 + (L_{22} + R_{22})J_2 \end{aligned} \quad (5)$$

where the operators are defined by

$$\begin{aligned} L_{11}f &= \frac{1}{2}f - \int_0^x G_{\mathbf{n}}(\mathbf{r}_1; \mathbf{r}'_1) f(\mathbf{r}'_1) dr'_1, & R_{11}f &= - \int_x^X G_{\mathbf{n}}(\mathbf{r}_1; \mathbf{r}'_1) f(\mathbf{r}'_1) dr'_1, \\ L_{12}f &= - \int_0^x G_{\mathbf{n}}(\mathbf{r}_1; \mathbf{r}'_2) f(\mathbf{r}'_2) dr'_2, & R_{12}f &= - \int_x^X G_{\mathbf{n}}(\mathbf{r}_1; \mathbf{r}'_2) f(\mathbf{r}'_2) dr'_2 \end{aligned} \quad (6)$$

with the obvious definitions for $L_{21}, L_{22}, R_{21}, R_{22}$. In these expressions the left-hand integrals L_{ii} are interpreted as the Cauchy principal value, and r'_i indicates integration along surface S_i .

Eqs. (5) can be expressed more concisely if we define the vectors \mathbf{u} and \mathbf{f} as the pairs of functions

$$\mathbf{u} = (J_1, J_2), \quad \mathbf{f} = (H_{inc}(\mathbf{r}_1), H_{inc}(\mathbf{r}_2)). \quad (7)$$

We can then write (5) in the form

$$\mathbf{f} = \mathbf{A}\mathbf{u} \equiv (\mathbf{L} + \mathbf{R})\mathbf{u} \quad (8)$$

where \mathbf{L} and \mathbf{R} are the 2×2 matrix operators whose entries are integral operators L_{ij}, R_{ij} corresponding to the above splitting (see ref []). \mathbf{L} therefore accounts for scattering from the left. The formal solution is given by

$$\mathbf{u} = (\mathbf{L} + \mathbf{R})^{-1}\mathbf{f}. \quad (9)$$

The main task is the inversion of $(\mathbf{L} + \mathbf{R})$. As in previous treatments [12] we make use of the assumption that the effect of \mathbf{R} is ‘small’ in some sense, reflecting the fact that most of the scattering is due to interaction from the left. The solution (9) can be then expanded in a series

$$\mathbf{u} = [1 - \mathbf{L}^{-1}\mathbf{R} + (\mathbf{L}^{-1}\mathbf{R})^2 - \dots] \mathbf{L}^{-1}\mathbf{f} \quad (10)$$

Provided it converges this equation can be truncated and treated term by term. When the system is discretized, the operator \mathbf{L} becomes a lower triangular matrix operator, whose entries are simply the four lower-triangular matrices arising from L_{ij} . Similarly \mathbf{R} becomes an upper triangular matrix operator in which the matrices are strictly upper triangular. Inversion of the matrix \mathbf{L} can be carried out very efficiently (using Gaussian elimination and backward substitution) to give the first term of eq.(10). Since subsequent terms in the series are products of \mathbf{L}^{-1} and \mathbf{R} , they can also be evaluated efficiently.

2.1.2 Numerical Solution

The main steps in the numerical treatment of the equations are to truncate the series, discretize the integral equation, and solve the resulting linear system. The details of the discretization itself are identical to those set out elsewhere [20] and need only be outlined briefly.

The series solution (10) can be regarded as an iterative solution, of which one or two terms are sufficient (see e.g. [19]). The first term gives say $\mathbf{u}_1 = \mathbf{L}^{-1}\mathbf{f}$. The first correction $\mathbf{u}_2 = \mathbf{L}^{-1}(\mathbf{R}\mathbf{u}_1)$ to this is calculated by applying the integral operator \mathbf{R} and inverting \mathbf{L} again, to give

$$\mathbf{u} \cong \mathbf{u}_1 - \mathbf{u}_2.$$

This gives the required surface currents along the waveguide boundaries, which is then used as the driving field for the calculation of interior fields, using eq. (2). To discretize we divide the integrals into evenly spaced subintervals, using around 10 points per wavelength. Each subintegral can be linearised and expressed approximately as a coefficient times the unknown function value. As an example, the L_{11} term in equation (6) can be written as a matrix equation, say

$$H_{inc} = AH. \quad (11)$$

in which the matrix A has entries

$$\begin{aligned} A_{mn} &= \frac{i\delta}{4}\sigma_n \left. \frac{\partial H_0^{(1)}}{\partial n} \right|_{kr_{mn}} \quad \text{for } m \neq n \\ A_{mm} &= - \left[\frac{1}{2} - \frac{\delta}{\sigma_m^2 \pi} s''(x_m) \right] \end{aligned} \quad (12)$$

where $\sigma_n = \sqrt{1 + s'(x_n)^2}$ is the slope variable where the prime denotes the x -derivative, $h' = dh/dx$, and the off-diagonal entries $m \neq n$ have simply been approximated by the Green’s function, with a factor accounting for arc-length.

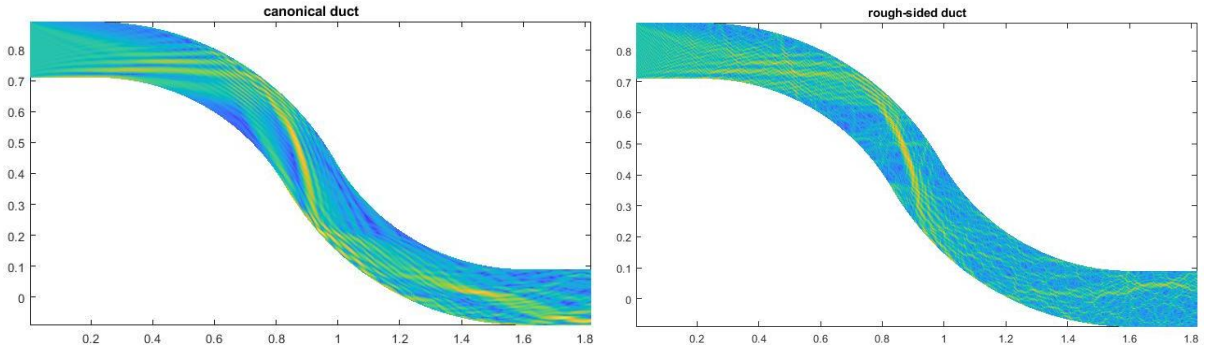


Figure 1: Canonical duct (left) compared with slightly rough duct, fine scale roughness (right)

2.1.3 Computational Results

The waveguide profile is specified by the addition of a continuous stochastic process $r(x)$, say, to a smooth (canonical) surface. The canonical shape chosen here is one for which the truncated series solution has been carefully validated [19]. Surface variation $r(x)$ is Gaussian distributed and is generated with chosen variance σ^2 (or r.m.s. height σ) and given autocorrelation function $\rho(\xi) = \langle r(x)r(x+\xi) \rangle$. The length scale of the variation along the duct wall can be characterised by the distance over which ρ decays by a factor of e^{-1} . (The roughness is statistically stationary so that ρ is a function of spatial separation ξ only.)

In the examples shown in Figure 1 the aperture A is at the left, the depth at A is 20λ , and the overall length with respect to x is 200λ , where λ is the wavelength. A plane wave is incident on the aperture, at an angle of 10° to the horizontal. This induces a surface current, and the resulting field amplitude internal to the duct is shown. The left-hand figure shows the smooth-sided duct and on the right is the rough-sided duct. In this case the scale size is around 0.01. It is seen here that even a small perturbation r leads to significant degradation of the pattern which would otherwise be observed. This highlights the importance of realistic modelling for such problems. It is this perturbation which allows reconstruction of the surface roughness profile.

Figure 2 shows the field intensity along two curves running along the duct adjacent and just above and below the axis.

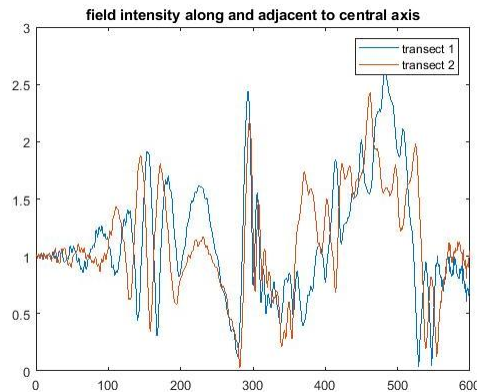


Figure 2: Measured field intensity along two curves adjacent to the canonical duct axis for the example of Fig. 1

We now consider the backscattered field or scattering cross-section, the variation with incident

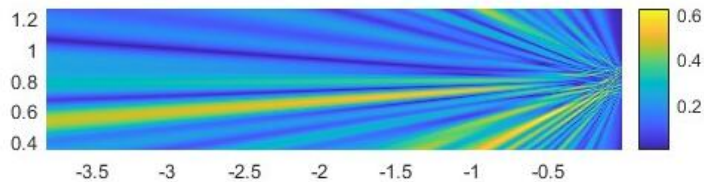


Figure 3: Backscatter due to 0° incident fields, rough duct: single realisation

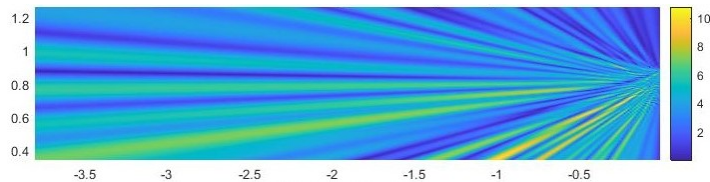


Figure 4: Backscatter due to 0° incident fields, rough duct: sum over 40 realisations

angle, and the effect of surface roughness upon this. Note that this is illustrative and not intended to be a full exploration of parameter space.

The backscatter fields are calculated as follows: The scattered component H_s of the field is obtained in the same way as the previous figures. The backscattered field in the region $x < 0$ results entirely from H_s across the aperture, since the remaining field H_{inc} is composed entirely of right-travelling waves. We can therefore calculate the external scattering cross-section by evaluating the Helmholtz-Kirchhoff integral of H_s at the aperture. (This is analogous to the procedure applied to obtain the incident field itself beyond the aperture.)

Figures 3 to 4 first show the spatial intensity pattern, including the near field, in order to illustrate the roughness effects, for a field incident normal to the aperture. The amplitude pattern has been scaled with distance from the aperture plane by applying a $1/\sqrt{x}$ factor to account for geometrical spreading. Figures 3, 4 show respectively a single realisation and the sum over multiple realisations. A striking feature which is seen here is the asymmetrical ‘ray’ in both coherent field and mean amplitude. In 5 we show the directivity pattern for a range of incident angles averaged over multiple realisations, compared side-by-side with the smooth duct case. These were obtained by first calculating the field and normal derivative at the aperture, and applying a far-field Helmholtz-Kirchhoff integration. It is interesting to note the persistent peak which occurs for all incident angles, but only in the presence of roughness, at around 120° , that is 40° from normal to the aperture. This peak may be regarded as a signature of the waveguide geometry which is enhanced by the roughness.

Recall that these calculations were done using the first two terms of the L-R series to produce the surface currents, followed by an ‘exact’ numerical surface integral. If only the first L-R term is used, the surface integral (roughly speaking) includes backscattered rays which do not interact with the surface; in other words it gives direct backscatter only. On the other hand, the second term allows for constructive interference between reversible ray paths; such paths cannot occur for direct backscatter (apart from specular).

We now consider a linear waveguide of varying cross-section.

2.2 Forward problem: Rough three-dimensional waveguide

The formal operator splitting solution described above generalises relatively straightforwardly to 3-dimensional ducts. In principle, in fact, it is more straightforward than in 2-dimensions since the coupled integral equations are replaced by a single, although higher-dimensional, integral equation. The

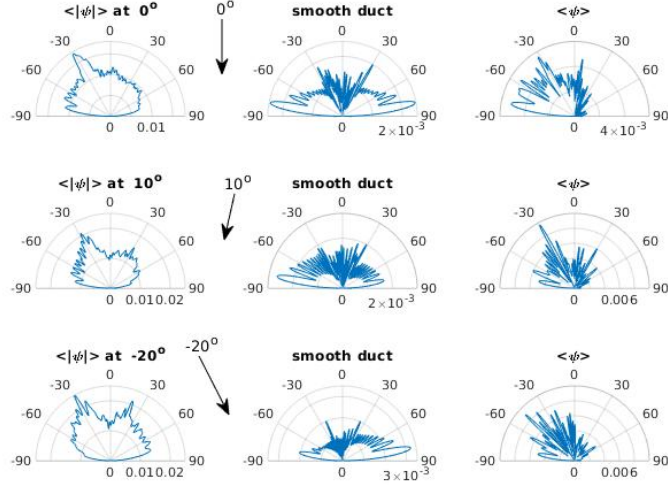


Figure 5: Directivity patterns for 3 incident angles, averaged over 50 realisations of rough duct showing mean amplitude (left), mean field (right), and corresponding pattern for zero roughness (middle).

main complication is in the numerical treatment, since there is a further horizontal direction transverse to the propagation direction; the lower triangular matrices of the previous section now become block-lower-triangular. Consequently, at *each* step in the marching procedure a matrix inversion is required. However, this is relatively fast, since that matrix dimension corresponds to the number of points around the duct circumference, rather than the much larger total number of unknowns. This has been described elsewhere. We describe this briefly in this section and give some numerical results.

For the perfectly conducting (PEC) case, the governing Stratton-Chu or magnetic field integral equations [MFIE] must be solved over the irregular boundary to obtain electric surface current \mathbf{J} ; this surface current is then used in a scattering integral to obtain the electromagnetic signature.

$$\mathbf{J}_{inc} = \frac{1}{2}\mathbf{J} - \mathbf{n} \times \int_{\text{surface}} \mathbf{J} \times \nabla G \, dS \quad (13)$$

We again tackle this problem using the Left-Right Splitting method (L-R), in which successive terms model increasing orders of multiple scattering.

We again write the above equation formally as $\mathbf{A}\mathbf{J} = \mathbf{J}_{inc}$, where \mathbf{J}_{inc} is the field incident (say) from the left, so that $\mathbf{J} = \mathbf{A}^{-1}\mathbf{J}_{inc}$. The inverse of \mathbf{A} can again formally be expressed as a series

$$\mathbf{A}^{-1} = \mathbf{L}^{-1} - \mathbf{L}^{-1}\mathbf{R}\mathbf{L}^{-1} + \dots \quad (14)$$

Discretization of the integral equation yields a block matrix equation, in which \mathbf{L} is the lower triangular part of the block matrix \mathbf{A} (including the diagonal) and \mathbf{R} is the upper triangular part. Under the assumption that most energy is right-going, \mathbf{L} is the dominant part of \mathbf{A} , and the series can be truncated to provide an approximation for \mathbf{J} . This approach has several advantages. In terms of wavelength λ , evaluation of each term scales with the fourth rather than the sixth power of λ required for \mathbf{A}^{-1} . Subsequent terms, of which typically only the first one or two are needed, each have the same computational cost. With further approximations this can be reduced to λ^3 . However, the low complexity and memory requirement allow very large problems to be tackled without such additional approximations. The algorithm also lends itself well to parallelisation, and the speed scales approximately linearly with the number of processors.

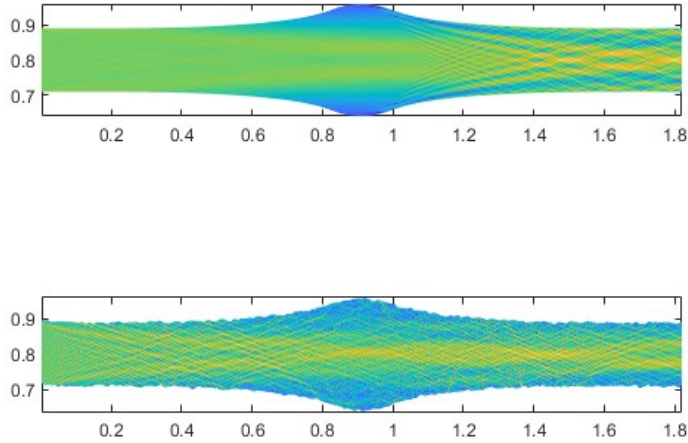


Figure 6: Intensity pattern in a smooth-sided and rough-sided waveguides of varying cross-section (respectively upper and lower plots, at zero degrees incidence)

2.2.1 Numerical Results

We present some examples for the 3-dimensional rough-sided waveguide. Figure 8 is a short section of around 34 wavelengths of a curved duct with moderate roughness. The aperture is 20 wavelengths in diameter and is illuminated by a vertically polarised 10GHz plane wave at 10° from the horizontal. The scattered component of the surface current amplitude induced by the incident field is shown. In Figure 9 is an example of the duct with more significant roughness, for the same incident field and aperture size. The section shown in both cases is around 34 wavelengths, and colour represents the surface current amplitude.

For this latter case, the resulting fields internal to the duct were calculated. Figure 10 shows the field intensity along a vertical plane running along the middle of the duct, i.e. the intersection of the (x, z) -plane with the duct. The field on a cross-section transverse to the propagation direction, i.e. parallel to the (y, z) -axis, is given in Figure 11,

Finally, shown in Figure 12, we calculate the surface currents on a larger duct of around 200 wavelengths, with the fields resulting from a 32GHz plane wave incident on the aperture.

3 Inverse problem: Reconstruction of waveguide surface

In this section we set out the principles of the marching method inverse solution which has been applied elsewhere, and formulated here in the context of an irregular waveguide. The intention is to express the algorithm in compact explicit form, which may be applied in multiple regimes, and which we expect to be amenable to convergence and regularisation analysis. The algorithm is not implemented here; this will be carried out in future work.

The approach is motivated by earlier work and is largely based on forward scattering assumptions and L-R operator expansion. Although we describe key quantities in terms of a waveguide, equations

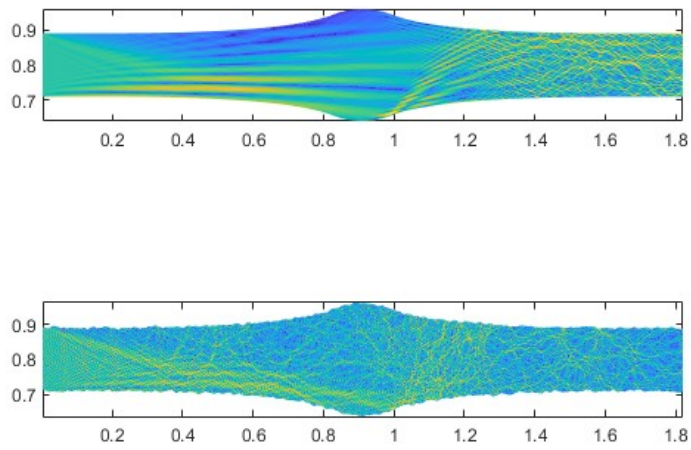


Figure 7: Intensity pattern in a smooth-sided and rough-sided waveguides of varying cross-section (respectively upper and lower plots, at a 10° angle of incidence directed downwards)

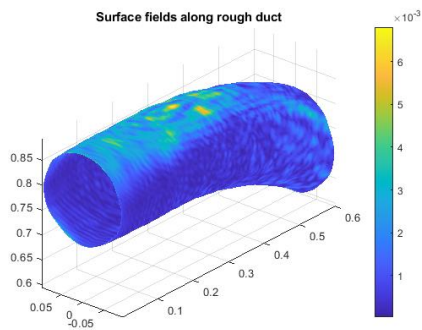


Figure 8: Slightly rough duct of length 34λ

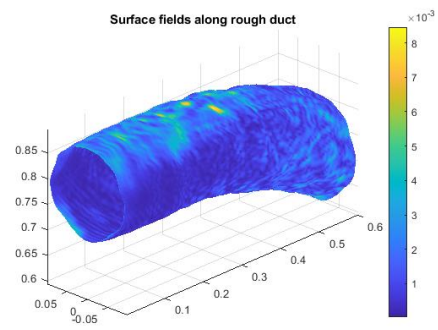


Figure 9: Rough duct, length 34λ

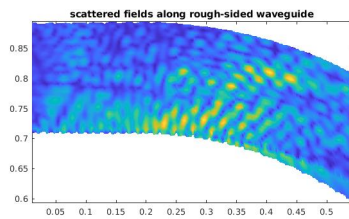


Figure 10: Duct length 34λ , 10GHz

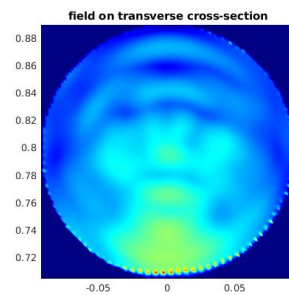


Figure 11: Duct length 34λ , 10GHz

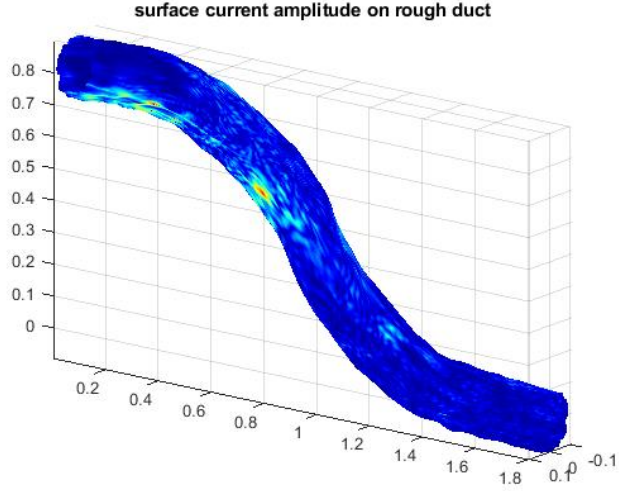


Figure 12: Surface current amplitude at 32GHz along rough duct

are derived in a more general setting in order to encompass various 2D and 3D geometries. The specific details for each implementation will depend closely on the geometry and the Green's function in each case.

Suppose $\mathbf{s} = \mathbf{s}(x, \phi)$ is the duct surface, where x is the horizontal component of the propagation direction and ϕ is a radial (or more generally transverse) coordinate. We will suppose that the underlying smooth (canonical) duct shape is known. We aim to recover the surface profile $\mathbf{s}(x, \phi)$ from the equations relating unknown surface fields (both incident and scattered) to the measured data. The main properties on which the method is based are as follows: The forward-scattering nature of the approximation allows us to reconstruct the solution sequentially, sweeping along the propagation direction x . In 2D settings [19] this has been found to be both efficient and remarkably robust, exhibiting a type of self-regularisation with respect to measurement noise. The incident field at $\mathbf{s}(x, \phi)$, depends only on $\mathbf{s}(x, \phi)$ itself; this allows use of an invertible transformation within the algorithm. The unknown surface field is approximated by its dependence on 'upstream' values, and crucially its dependence on 'local' surface values is weak (in a sense to be discussed).

Let $\mathbf{w}(x)$ represent the scattered field measured along the central axis of the duct. At each x this will consist of a vector of N_ϕ values where N_ϕ is the number of points we wish to recapture around the duct at each distance x , which for simplicity will be assumed constant in x . We will assume a known underlying 'canonical' duct shape. (For an extended surface varying about a plane N_ϕ would represent the number of points transverse to the propagation direction. For a rough 2D duct, $N_\phi = 2$, and for a rough surface in 2D $N_\phi = 1$.)

Let $\mathbf{u}(x, \phi)$ be the unknown surface field. When discretized this will again become a vector, of size N_ϕ for each $x = x_i$, where $i = 1, \dots, n$. The x -values are again assumed evenly spaced; this is for convenience and is not an inherent limitation of the proposed algorithm. Let $\mathbf{v}(\mathbf{s}(x, \phi))$ be the incident field along the surface, considered as a function of x . Applying the series solution to the coupled integrals and taking only the first term, i.e. using $\mathbf{A} \cong \mathbf{L}$, $\mathbf{A}^{-1} \cong \mathbf{L}^{-1}$ gives

$$\begin{aligned} \mathbf{u}(x, \phi) &\cong \mathbf{L}^{-1} \mathbf{v} \\ \mathbf{w}(x, \phi) &\cong \mathbf{L} \mathbf{u} \end{aligned} \tag{15}$$

All terms here including the operators depend on the unknown rough profile. We will suppose that the duct aperture $\mathbf{s}(0, \phi)$ is known.

Denote by $\mathbf{S}, \mathbf{U}, \mathbf{W}, \mathbf{V}$ the discretized forms corresponding respectively to $\mathbf{s}, \mathbf{u}, \mathbf{w}$, and \mathbf{v} , over the whole computational domain, so that \mathbf{U}, \mathbf{W} and \mathbf{V} all depend on \mathbf{S} . Denote by $\mathbf{S}_i, \mathbf{U}_i, \mathbf{W}_i, \mathbf{V}_i$ the vectors of length N_ϕ evaluated at distance x_i . In equations (15), $\mathbf{u}(x, \phi)$, $\mathbf{w}(x, \phi)$ and operators $\mathbf{L}^{-1}, \mathbf{L}$ evaluated at x depend only on upstream values $\mathbf{s}(X \leq x, \phi')$ so we can write

$$\begin{aligned}\mathbf{U}_i &= \sum_{j=1}^i M_{ij} \mathbf{V}_j \\ \mathbf{W}_i &= \sum_{j=1}^i N_{ij} \mathbf{U}_j\end{aligned}\tag{16}$$

where M_{ij} and N_{ij} are transformations derived from the operators in (15). Suppose that at step x_i we have already obtained the surface values at all range steps x_j for $j < i$. We therefore rearrange this to obtain coupled equations

$$\begin{aligned}\mathbf{U}_i - M_{ii} \mathbf{V}_i &= \sum_{j=1}^{i-1} M_{ij} \mathbf{V}_j \\ \mathbf{W}_i - N_{ii} \mathbf{U}_i &= \sum_{j=1}^{i-1} N_{ij} \mathbf{U}_j\end{aligned}\tag{17}$$

in which the left-hand-side is unknown, while the terms on the right are known. The quantities M_{ii}, N_{ii} are N_ϕ -dimensional matrices. We have thus reduced the problem to that of expressing the LHS explicitly in terms of the, as yet unknown, values $\mathbf{S}_i \cong s(x, \cdot)$.

The above considerations and equations (17) encompass the inverse problem for the 3D duct and the rough surface in 3D, the 2D duct ($N_\phi = 2$) and the rough surface in 2D ($N_\phi = 1$). It is instructive to revisit the 2D problem, for which a similar approach was used: Consider an irregular 1-dimensional surface. Here the scattered field w is measured along a line parallel to the mean plane. To simplify notation we rewrite this as:

$$\begin{aligned}u_i - \alpha_i v_i &= \sum_{j=1}^{i-1} \alpha_{ij} v_j \\ w_i - \beta_i u_i &= \sum_{j=1}^{i-1} \beta_{ij} u_j\end{aligned}\tag{18}$$

Each term on the left is now a scalar. The values α_i and β_i , depend in a known way on the surface but it is found [21, 22] that they may be approximated by their values at the canonical flat surface. The measured data point is w_i , and the incident field v_i can be approximated linearly in terms of the unknown surface height $s(x_i)$, say $v_i = \gamma_i s_i$. This results in a pair of equations in the two unknowns u_i, s_i which we can write as

$$\begin{aligned}u_i - \alpha_i \gamma_i s_i &= \sum_{j=1}^{i-1} \alpha_{ij} v_j \\ \beta_i u_i &= w_i - \sum_{j=1}^{i-1} \beta_{ij} u_j\end{aligned}\tag{19}$$

This system is overdetermined since u_i depends on s_i and in previous work this issue has been circumvented in various ways [12, 14]. Here we initially treat u and s as locally independent, and note that second equation (19) contains only u_i ; we can therefore solve for u_i and substitute into the upper equation (19) to find s_i . [To summarise the rationale for this: u_i depends on s_j for *all* $j \leq i$; the dependence of u_i 'locally' on s_i is therefore weak, and s_i can be replaced by its canonical or mean surface value at x_i .]

We thus obtain the marching solution:

$$s_i = \frac{-1}{\alpha_i \gamma_i} \left\{ \sum_{j=1}^{i-1} \alpha_{ij} v_j - \frac{1}{\beta_i} \left[w_i - \sum_{j=1}^{i-1} \beta_{ij} u_j \right] \right\}\tag{20}$$

This gives the solution in the case of a rough surface varying about a mean plane in 2D. It can be refined by iterative improvement to take into account the interdependence between surface profile and the resulting wavefields. An initial guess or assumption is needed for the value s_1 , but the system has been found very robust with respect to this choice. The forward scatter assumption can also be relaxed, although this is less straightforward as it is highly regime-dependent.

Returning to the more general case, an analogous higher-dimensional procedure can be applied: In equation (20), the term γ_i remains a scalar. However, α_i and β_i become $N_\phi \times N_\phi$ matrices; the reciprocals become matrix inverses, to be evaluated at each step x_i . This yields:

$$\mathbf{S}_i = \frac{-1}{\gamma_i} M_{ii}^{-1} \left\{ \sum_{j=1}^{i-1} M_{ij} \mathbf{V}_j - N_{ii}^{-1} \left[\mathbf{w}_i - \sum_{j=1}^{i-1} N_{ij} \mathbf{U}_j \right] \right\} \quad (21)$$

It should be emphasized that the dimensions of matrices to be inverted here are relatively small, so that the algorithm is computationally tractable. Indeed the computational cost is broadly comparable with that of the L-R series for the forward problem.

The above formulation assumed that data is measured and surface reconstruction is required at the same (evenly-spaced) values of x . It was also assumed implicitly that the data were arranged parallel to the surface; that is along the duct axis, or on a plane parallel to the mean plane in the extended surface case. Neither of these assumptions is an inherent limitation and both can be relaxed, provided the number of available data points is not reduced. However, since the scattered wave is forward-going, the optimal measurement location with respect to distance from the surface depends on the angle and spread of the incident wave. This issue was not critical in previous applications because of the robustness and self-regularising characteristics with respect to measurement noise, but it should ideally be taken into account.

4 Conclusions

In this paper we have, first, calculated wave scattering inside rough-sided ducts, and both 2- and 3-dimensional example geometries, by the operator expansion method of Left-Right splitting. This utilizes the predominance of forward scatter but allows the calculation of multiple-scattering backscatter. For the 2-dimensional case we have examined mean directivity patterns for various angles. These patterns arise from the second term of the L-R series which captures the dominant multiple backscattering contributions.

We then derived a marching solution of the inverse problem, that is the recovery of the surface profile from measured data. This was expressed in terms of the waveguide, but is applicable for a range of geometries having a principal wave propagation direction, This marching or ‘surface sweep’ method recovers the surface values sequentially at successive points along the surface. The approach makes use of the first approximation to the L-R series solution, and is an explicit method, apart from coefficients which will depend on the specific geometry. This is not implemented here. The application to particular cases including the waveguide will be given in future work.

It may be observed that this raises the possibility of tackling an important dual inverse problem: the design of a boundary profile for a given incident field which will produce a given reflectivity pattern.

A long-term goal is to solve the surface reconstruction problem for a three-dimensional lined duct. In such geometries, even the forward problem, which is required for almost all inverse calculations, can be problematic because of prohibitive computational costs. This problem will be treated in future work based on the fast forward solver used here.

Acknowledgments

The authors are grateful to Yuxuan Chen for numerous helpful discussions. MS gratefully acknowledges support for this work under ONR NICOP grant N62909-19-1-2128.

References

- [1] RJ Wombell and John A DeSanto. The reconstruction of shallow rough-surface profiles from scattered field data. *Inverse Problems*, 7(1):L7, 1991.
- [2] Gang Bao and Lei Zhang. Shape reconstruction of the multi-scale rough surface from multi-frequency phaseless data. *Inverse Problems*, 32(8):085002, 2016.
- [3] Ali Yapar, Ozgur Ozdemir, Hulya Sahinturk, and Ibrahim Akduman. A newton method for the reconstruction of perfectly conducting slightly rough surface profiles. *IEEE transactions on antennas and propagation*, 54(1):275–279, 2006.
- [4] Mehmet Cayoren, Ibrahim Akduman, Ali Yapar, and Lorenzo Crocco. Shape reconstruction of perfectly conducting targets from single-frequency multiview data. *IEEE Geoscience and Remote Sensing Letters*, 5(3):383–386, 2008.
- [5] Ibrahim Akduman, Rainer Kress, and Ali Yapar. Iterative reconstruction of dielectric rough surface profiles at fixed frequency. *Inverse Problems*, 22(3):939, 2006.
- [6] Bo Zhang and Haiwen Zhang. Imaging of locally rough surfaces from intensity-only far-field or near-field data. *Inverse Problems*, 33(5):055001, 2017.
- [7] Karl F Warnick and Weng Cho Chew. Numerical simulation methods for rough surface scattering. *Waves in Random Media*, 11(1):R1–R30, 2001.
- [8] Fenglong Qu, Bo Zhang, and Haiwen Zhang. A novel integral equation for scattering by locally rough surfaces and application to the inverse problem: The Neumann case. *SIAM Journal on Scientific Computing*, 41(6):A3673–A3702, 2019.
- [9] Jianliang Li, Jiaqing Yang, and Bo Zhang. A linear sampling method for inverse acoustic scattering by a locally rough interface. *Inverse Problems and Imaging*, 15(5):1247–1267, 2021.
- [10] Ahmet Sefer, Ali Yapar, and Tanju Yelkenci. Imaging of rough surfaces by rtm method. *IEEE Transactions on Geoscience and Remote Sensing*, 2024.
- [11] Ahmet Sefer and Ali Yapar. An iterative algorithm for imaging of rough surfaces separating two dielectric media. *IEEE Transactions on Geoscience and Remote Sensing*, 59(2):1041–1051, 2020.
- [12] M Spivack. Direct solution of the inverse problem for rough surface scattering at grazing incidence. *Journal of Physics A: Mathematical and General*, 25(11):3295, 1992.
- [13] Yuxuan Chen and Mark Spivack. Rough surface reconstruction at grazing angles by an iterated marching method. *JOSA A*, 35(4):504–513, 2018.
- [14] Yuxuan Chen, Orsola Rath Spivack, and Mark Spivack. Rough surface reconstruction from phaseless single frequency data at grazing angles. *Inverse Problems*, 34(12):124002, 2018.
- [15] P Tran. Calculation of the scattering of electromagnetic waves from a two-dimensional perfectly conducting surface using the method of ordered multiple interaction. *Waves in Random Media*, 7(3):295–302, 1997.

- [16] David A Kapp and Gary S Brown. A new numerical method for rough-surface scattering calculations. *IEEE Transactions on Antennas and Propagation*, 44(5):711, 1996.
- [17] M Rodriguez Pino, Luis Landesa, Jose L Rodriguez, Fernando Obelleiro, and Robert J Burkholder. The generalized forward-backward method for analyzing the scattering from targets on ocean-like rough surfaces. *IEEE Transactions on Antennas and Propagation*, 47(6):961–969, 1999.
- [18] O Rath Spivack and M Spivack. Efficient boundary integral solution for acoustic wave scattering by irregular surfaces. *Engineering Analysis with Boundary Elements*, 83:275–280, 2017.
- [19] M Spivack, A Keen, J Ogilvy, and C Sillence. Validation of left–right method for scattering by a rough surface. *Journal of Modern Optics*, 48(6):1021–1033, 2001.
- [20] M Spivack, J Ogilvy, and C Sillence. Electromagnetic propagation in a curved two-dimensional waveguide. *Waves in Random Media*, 12(1):47–62, 2002.
- [21] M Spivack. A numerical approach to rough-surface scattering by the parabolic equation method. *J. Acoust. Soc. Am.*, 87(5):1999–2004, 1990.
- [22] M Spivack. Moments of wave scattering by a rough surface. *The Journal of the Acoustical Society of America*, 88(5):2361–2366, 1990.